SI METHODS

Animals

Animal manipulation protocols were approved by the institutional ethics committee of the University of Quebec at Montreal (*Comité institutionnel de protection des animaux* (CIPA); Reference number: 650). For epistasis studies, *Toupee*$^{Tg/Tg}$ females (FVB/N background) and *Chd7*$^{Gt/+}$ males (C57BL/6-Sv129 mixed background) were intercrossed to generate *Toupee*$^{Tg/+}$;*Chd7*$^{Gt/+}$ double heterozygotes and corresponding *Toupee*$^{Tg/+}$ single heterozygotes. *Chd7*$^{Gt/+}$ single heterozygotes on the same hybrid background were generated by crossing the same *Chd7*$^{Gt/+}$ males with wild-type FVB/N females.

For olfactory tests, after proper familiarization to the test conditions, mice were individually placed in a clean cage and exposed to a small piece of Whatman paper containing 100µl of water or 100µl of C57BL/6 urine (10^{-2} dilution in water) during 2 min for each, with a 2 min interval between each exposition. The total number and cumulative duration of sniff bouts were recorded in order to express results as mean elapsed time per sniff bout.

Image acquisition

Image acquisition was performed with a Leica DFC 495 camera (for color images) or a Lumenera Infinity 2.0 camera (for black and white images) mounted on a Leica M205 FA stereomicroscope, with the exception of immunofluorescence analyses which were imaged with a Nikon A1 laser scanning confocal microscope. Image processing and analysis was all done with the ImageJ software, including for cell counting, measurement of choroidal fissure width as well as analysis of migration speed and persistence (see below). For Pearson correlation analysis, relevant images were deconvoluted and analyzed with the AutoQuant 3X program.

Ex vivo time-lapse imaging of NCCs

The posterior end of an e10.5 embryo (obtained from G4-RFP or *Toupee*$^{Tg/Tg}$;G4-RFP intercrosses) containing pre-migratory NCCs was cut transversely behind the hindlimb bud and deposited on a small nitrocellulose filter (Millipore GSWP01300) so that a lateral side is attached to the filter and the other side is free to be imaged. The filter paper was then flipped (with tissue side down) onto paraffin rods streaked in parallel on a 60-mm cell culture dish (Corning). The samples were cultured in DMEM/F12 containing 10% FBS and penicillin/streptomycin, and incubated in a microscope incubation chamber (Okolab) under standard conditions (37°C, 5% CO_2) during 15h while 600 µm-thick stacks were acquired every 10 min (Nikon A1R confocal unit; 10X objective). Only NCCs migrating ventrally through the anterior half of somites were taken into account. Average speed (total tracked distance divided by total time) and persistence (straight line from start to finish divided by total tracked distance) were calculated from 40-min periods.

FACS

Embryonic tissues (whole e10.5 embryos for RNAseq; heads and trunks of e10.5, e13.5 and e16.5 embryos for RT-qPCR) obtained from G4-RFP or *Toupee*$^{Tg/Tg}$;G4-RFP intercrosses were dissociated at 37°C with 1.3 mg/ml dispase II, 0.4 mg/ml collagenase and 0.1 mg/ml DNAse I in EMEM medium. For each biological replicate, between 240,000-300,000 RFP+ and RFP- cells (from a total of 6-8 embryos at e10.5 or 1-2 embryos at e13.5 and e16.5) were collected using the BD FACSJazz cell sorter (BD Biosciences) and stored at -80°C until RNA extraction.

High throughput genome and transcriptome sequencing

Whole genome and transcriptome sequencing was performed at McGill University and Génome Québec Innovation Centre. This included library generation, sequencing using the HiSeq 2500 platform (Illumina) and bioinformatics analysis. For RNAseq, ribosomal RNA-depleted libraries (using 120 ng of total RNA as starting material) were generated and sequenced for three biological replicates per genotype (G4-RFP *vs* *Toupee*$^{Tg/Tg}$;G4-RFP) but only two per genotype met quality criteria for subsequent bioinformatics analysis. Paired-end sequences of 100-bp in length (215 million reads for the genomic DNA and between 51-84 million reads per transcriptome sample) were mapped onto the mm10 *Mus musculus* reference genome.

Cell culture and transfection

For primary culture of e10.5 embryonic cells, whole embryos were dissociated as described above for FACS and the resulting cell suspension (10^{-1} dilution in EMEM medium) was plated on gelatin-coated coverslips in 6-well plates. Dissociated cells were cultured in EMEM medium containing 10% FBS and penicillin/streptomycin under standard conditions (37°C and 5% CO_2).

Co-IP, RIP, ChIP and RNA-ChIP

Co-IPs were performed in defined buffer (20 mM Tris pH 8.0, 1 mM EGTA, 1.5 mM MgCl2, 1 mM DTT, 1% Triton TX-100, 10% Glycerol, 1X Roche Complete protease inhibitors), containing either 25 or 200 mM NaCl. For untargeted ChIP and RIP experiments, cross-linked Neuro2a cells (using 1% PFA) were sonicated either in nuclear lysis buffer (50 mM Tris-HCl pH 8.0, 10 mM EDTA, 1% SDS, 1X Roche Complete protease inhibitors) for ChIP or in RIPA buffer (50 mM Tris-HCl pH 7.4, 2 mM EDTA, 150 mM NaCl, 1% NP-40, 0.5% Na-deoxycholate, 0.1% SDS, 1X Roche Complete protease inhibitors) for RIP. The nucleic acid content of purified ChIP and RIP samples was then assessed via Qubit fluorometric quantitation (ThermoFisher Scientific). For targeted ChiP and RNA-ChIP experiments, Neuro2a cells were treated with either vehicle (DMSO) or 25ng/ml Phorbol 12-myristate 13-acetate (PMA) for 4 hours. For RNA-ChIP, immunoprecipitated samples were also treated with 100 µg/ml DNAse I during 2 hours at 4°C, followed by RNA extraction and reverse transcription.

MBP fusion proteins and serine hydrolase assay

MBP, $_{MBP}$Fam172a and $_{MBP}$Fam172a^{S294A} proteins were produced in BL21 bacteria via IPTG (0.3 mM) induction of relevant pMAL-c5X constructs. Bacterially-produced proteins were then purified via amylose affinity chromatography and eluted with column buffer (20 mM Tris-HCl pH7.4, 200 mM NaCl, 1 mM EDTA, 1X Roche Complete protease inhibitors) supplemented with 100 mM maltose. For serine hydrolase assay, each protein sample (7.5 µg) was mixed with the probe, incubated at room temperature in the dark for 30 minutes and migrated on a 10% SDS-polyacrylamide gel.

Affinity purification coupled to tandem mass spectrometry analysis

Neuro2a cell extracts were fractionated using buffer conditions specific to each fraction: cytoplasm (10 mM Tris-HCl pH 8.0, 0.34 M sucrose, 3 mM $CaCl_2$, 2 mM MgOAc, 0.1 mM EDTA, 0.5% NP-40, 1 mM DTT and 1X Roche Complete protease inhibitors), nucleoplasm (20 mM Hepes pH 7.9, 1.5 mM $MgCl_2$, 150 mM KOAc, 3 mM EDTA, 10% glycerol, 0.1% NP-40, 1 mM DTT and 1X Roche Complete protease inhibitors) and chromatin (150 mM Hepes pH 7.9, 1.5 mM $MgCl_2$, 150 mM KOAc, 10% glycerol, 15 U/ml Benzonase, 0.44 U/ml RNAse A, 6.25 U/ml DNAse I, 1X Roche Complete protease inhibitors). Each

Neuro2a cell fraction (1.25mg) was passed on an amylose resin column containing immobilized $_{MBP}$Fam172a or MBP alone. Following extensive washing, interacting proteins were co-eluted with $_{MBP}$Fam172a or MBP as described above for the purification of MBP fusion proteins. Eluates were then individually precipitated using 72% TCA, 0.075% Na-deoxycholate and 2.5X Tris-EDTA. Preparation of trypsic fragments, LC-MS/MS analysis on a LTQ Orbitrap Fusion Tribrid mass spectrometer (ThermoFisher Scientific) and peptide identification were performed at the Proteomics Discovery Platform of the *Institut de recherches cliniques de Montreal* (IRCM). Proteins identified via at least one peptide (with probability greater than 90%) were accepted as $_{MBP}$Fam172a interactors if they were enriched at least 1.5-fold in comparison to the MBP negative control and detected in at least two out of the three biological replicates per fraction.

Figure S1

A

Genotype	Number of Mice	Ratio (%)
WT	96	24%
Toupee$^{Tg/+}$	221	54%
Toupee$^{Tg/Tg}$	85	22%

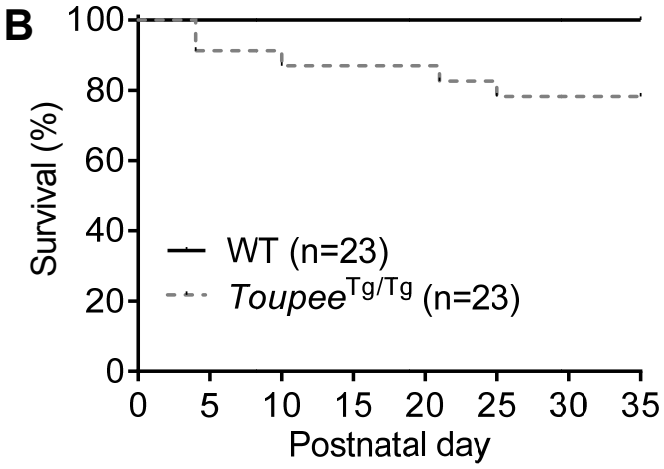

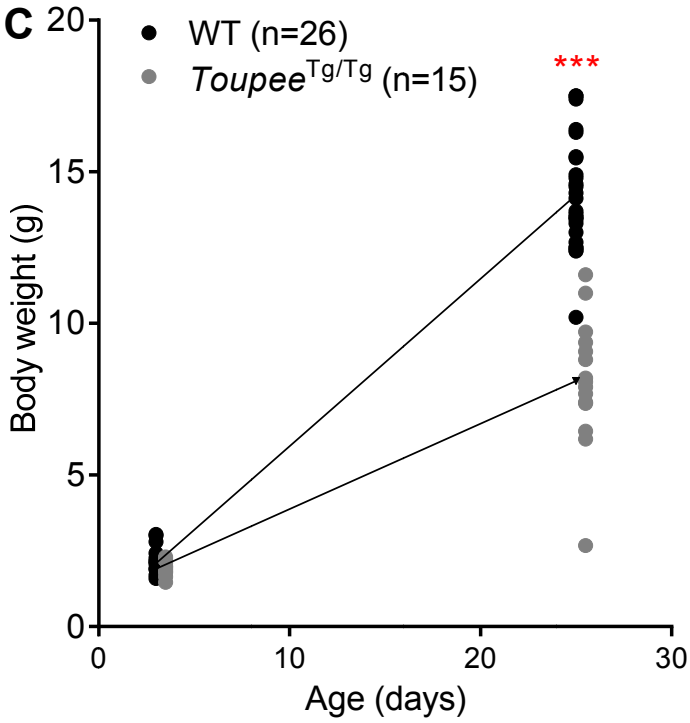

Figure S1. Early death and growth retardation in *Toupee*$^{Tg/Tg}$ mice. (A) Genotype distribution of offspring from *Toupee*$^{Tg/+}$ intercrosses (n=48 couples) at weaning. **(B)** Kaplan-Meier survival curve for WT and *Toupee*$^{Tg/Tg}$ mice. **(C)** Body weight comparison of WT and *Toupee*$^{Tg/Tg}$ mice at P3 and P25.

Figure S2

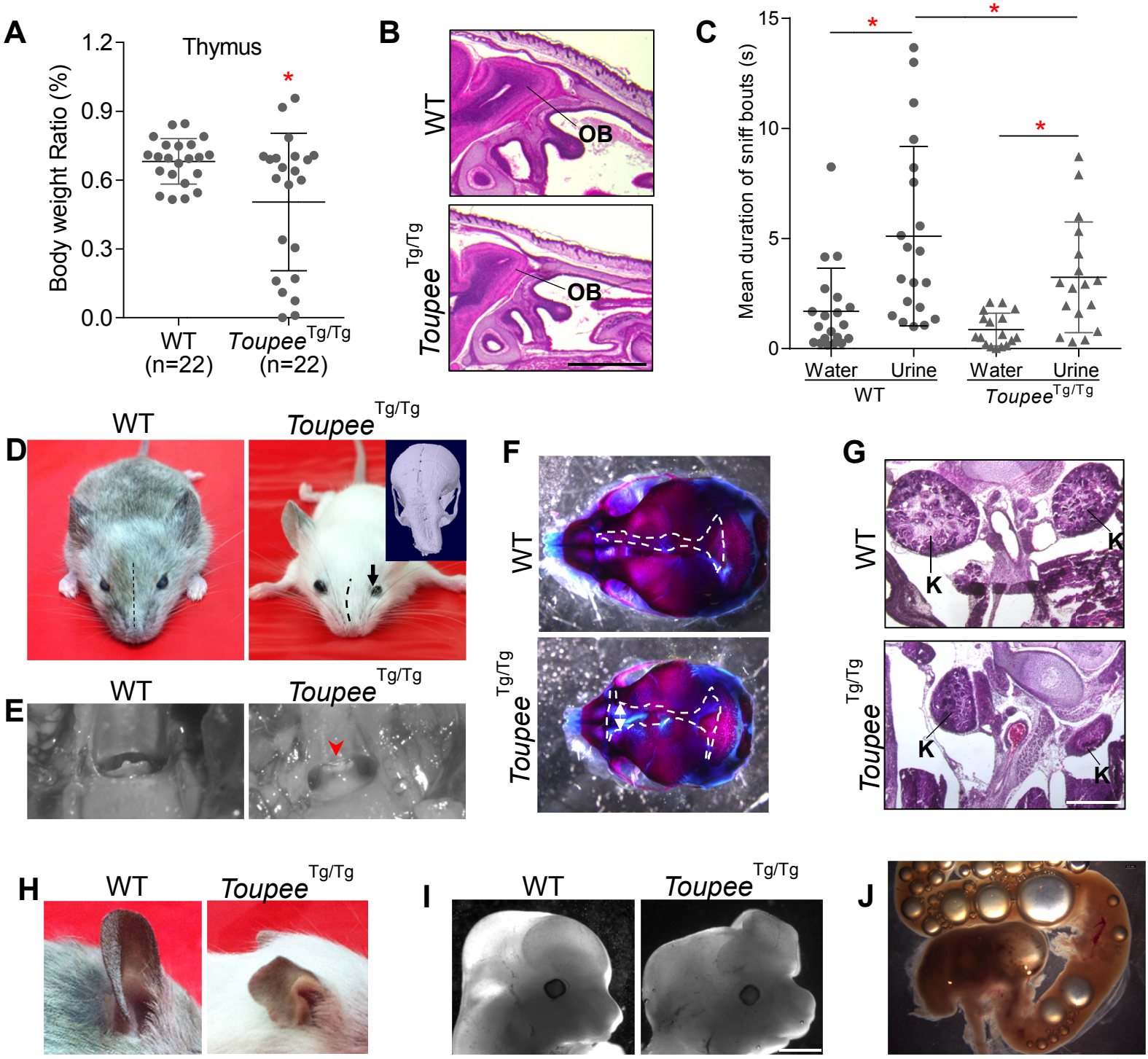

Figure S2. Less frequently observed minor features of CHARGE syndrome in *Toupee*$^{Tg/Tg}$ mice. (A) A subset of *Toupee*$^{Tg/Tg}$ mice exhibits a lower thymus/body weight ratio at P25. **(B)** H&E-stained sagittal sections of e18.5 heads (n=10 per genotype) revealing olfactory bulb hypoplasia in a subset of *Toupee*$^{Tg/Tg}$ embryos. **(C)** Results of olfaction tests (n=20 mice per genotype) showing that adult *Toupee*$^{Tg/Tg}$ mice are less efficient than WT mice at distinguishing urine from water. **(D)** A subset of *Toupee*$^{Tg/Tg}$ mice displays facial asymmetry including unilateral eyelid ptosis (arrow) and twisted facial bones (see µCT scan in the inset). **(E)** Frontal view of the oropharynx at P25 showing partial atresia (arrowhead) in a *Toupee*$^{Tg/Tg}$ animal. **(F)** Alizarin red and alcian blue double-stained e18.5 skulls (n=10 per genotype) showing that closure of the fontanelles (delineated by dashed lines) is delayed in a subset of *Toupee*$^{Tg/Tg}$ embryos (double-headed arrow). **(G)** H&E-stained cross-sections of e15.5 embryos showing kidney (K) hypoplasia in a *Toupee*$^{Tg/Tg}$ animal. **(H)** The outer ear of *Toupee*$^{Tg/Tg}$ animals is occasionally malformed. **(I)** Lateral view of e12.5 heads demonstrating exencephaly in a *Toupee*$^{Tg/Tg}$ embryo. **(J)** Gastrointestinal track of a P24 *Toupee*$^{Tg/Tg}$ animal filled with air bubbles. * $P \leq 0.05$ (Student's *t*-test). Scale bar: 1mm (B), 500µm (G).

Figure S3

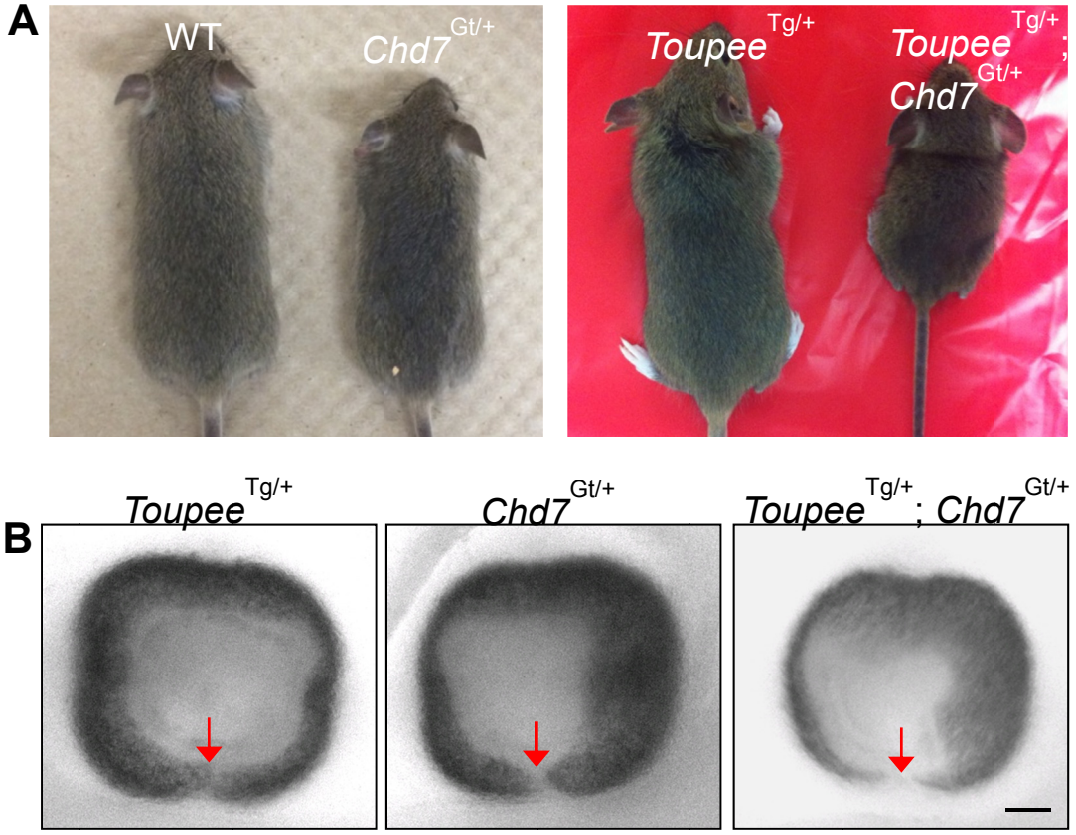

Figure S3. Genetic interaction between *Toupee*^{Tg} and *Chd7*^{Gt} alleles. (A) *Toupee*$^{Tg/+}$;*Chd7*$^{Gt/+}$ double mutants are markedly smaller than corresponding single mutants at P25. **(B)** Representative bright field images of e12.5 eyes showing that the choroidal fissure (red arrows) is wider in double mutant embryos. Scale bar: 50μm.

Figure S4

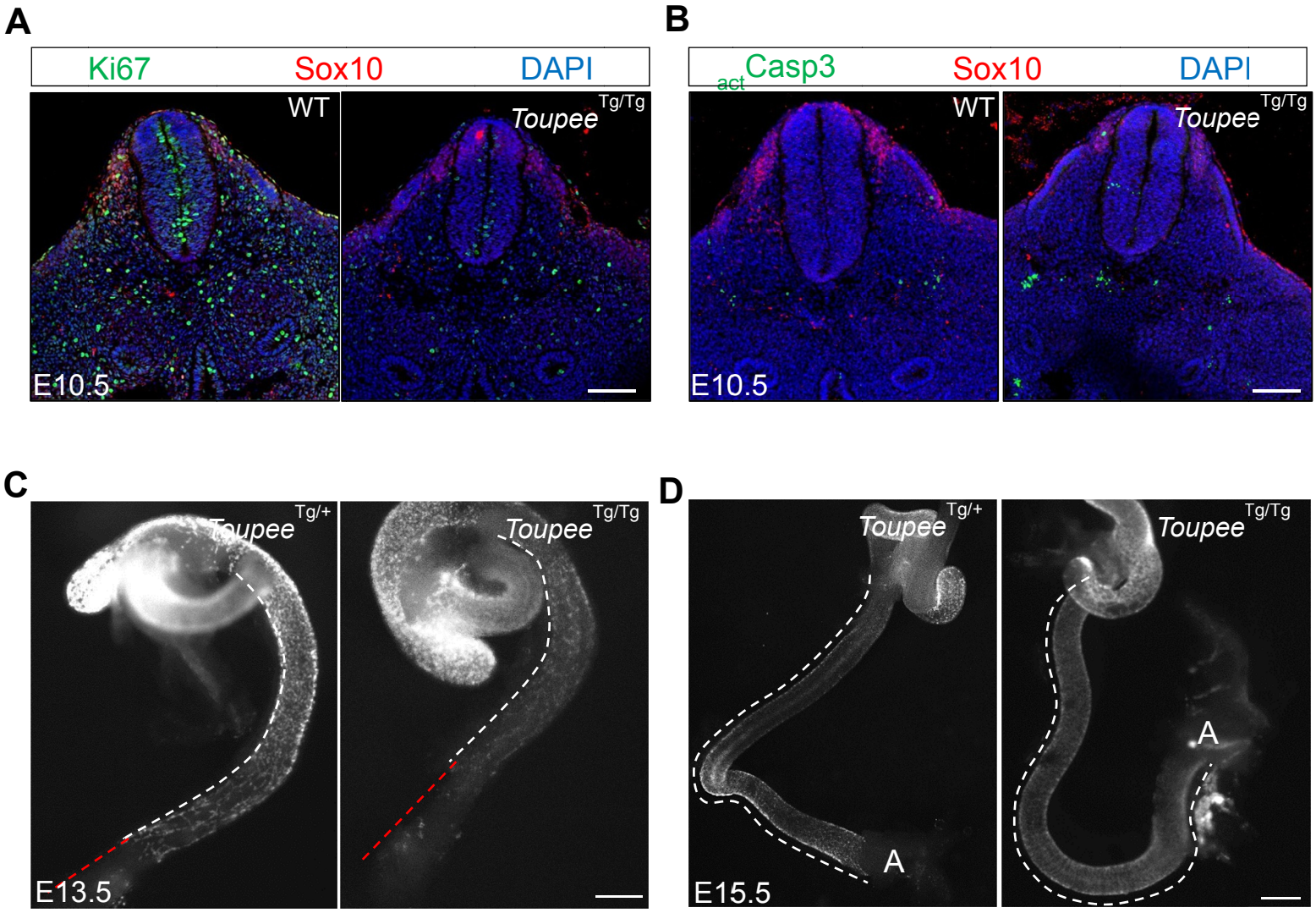

Figure S4. Defective NCC proliferation, survival and migration in *Toupee*$^{Tg/Tg}$ embryos. (A-B) Representative immunofluorescence images used for quantification of NCC proliferation and survival in Fig.2A-B (n=9 per genotype). Cross-sections (30µm) of e10.5 embryos at the level of the hindlimb bud were double-labeled with anti-Sox10 (red) and anti-Ki67 or anti-activated Caspase3 (green), and counterstained with DAPI (blue). **(C-D)** Representative images used for quantification of hindgut colonization by fluorescently labeled (owing to G4-RFP transgene) enteric NCCs in Fig.2E. The white dashed lines delineate the colonized hindgut segment, whereas the red dotted lines delineate the uncolonized hindgut segment (for each developmental stage, n=5 per genotype). Scale bars: 100µm (A-B), 500µm (C) and 1mm (D).

Figure S5

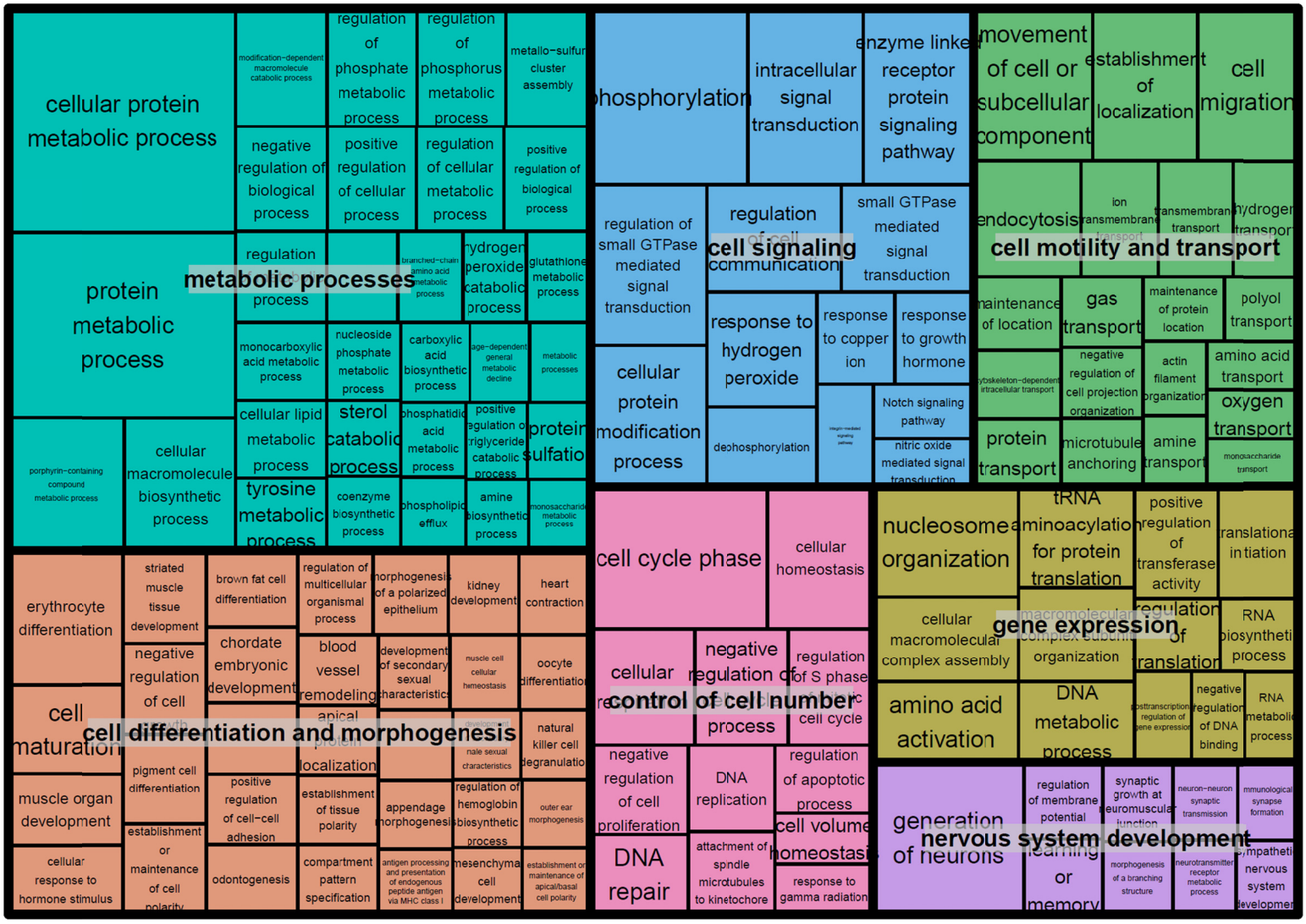

Figure S5. Enriched GO terms associated with the differentially expressed genes in *Toupee*$^{Tg/Tg}$ NCCs. REVIGO TreeMap representation of the GO analysis of the 3488 modulated genes displayed in Fig.2F. The 132 enriched terms (ontology level ≥ 5 and $P < 0.05$) are distributed into 7 main categories: Metabolic processes; Cell differentiation and morphogenesis; Cell signaling; Cell motility and transport; Control of cell number; Gene expression; and Nervous system development. Size of boxes is proportional to statistical significance.

Figure S6

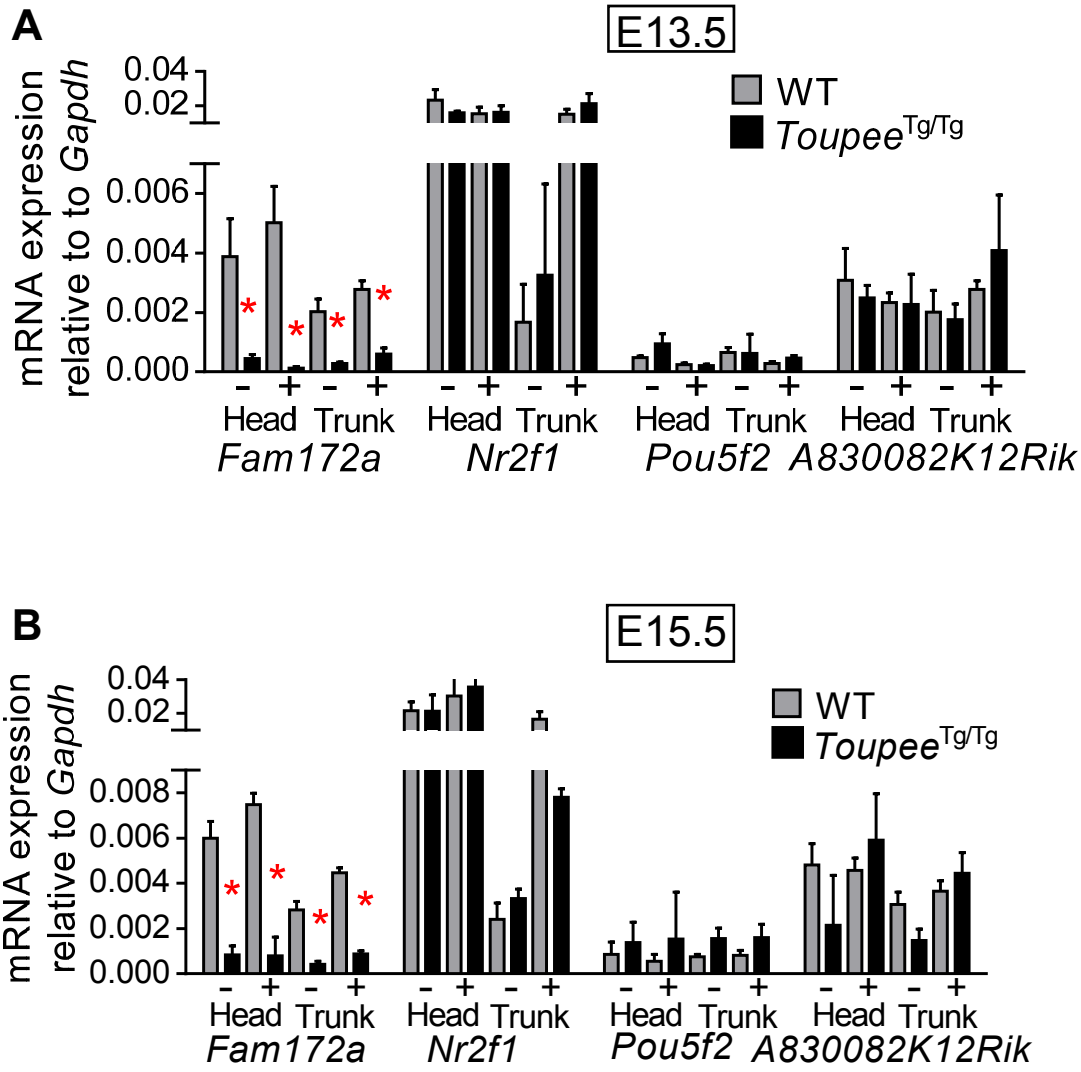

Figure S6. Specific downregulation of *Fam172a* expression in *Toupee*$^{Tg/Tg}$ embryos. RT-qPCR analyses of gene expression in *G4-RFP* (WT) and *Toupee*$^{Tg/Tg}$*;G4-RFP* (*Toupee*$^{Tg/Tg}$) embryos at e13.5 (A) and e15.5 (B). Transcript levels of *Fam172a*, *Pou5f2*, *Nr2f1* and *A830082k12Rik* were monitored in FACS-recovered NCCs (+) and non-NCCs (-) from the head and the trunk (n=3 per condition). Expression levels were normalized relative to *Gapdh*. * $P \leq 0.05$.

Figure S7

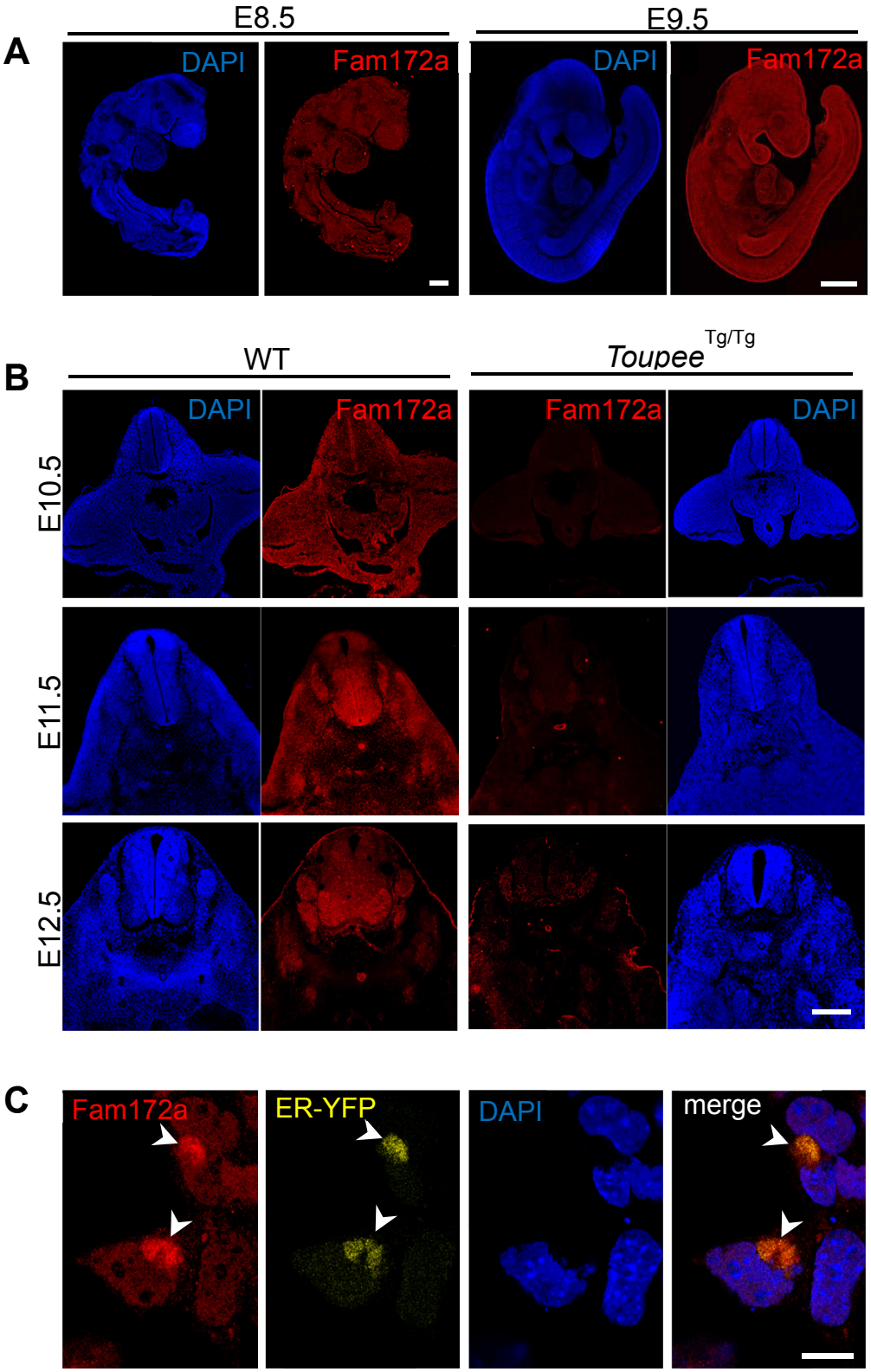

Figure S7. Analysis of Fam172a protein distribution in mouse embryos and COS7 cells. (A-B) Immunofluorescence analysis of the Fam172a protein in e8.5-9.5 WT embryos (A) and in cross-sections of e10.5-12.5 WT and *Toupee*$^{Tg/Tg}$ embryos (B) at hindlimb level (n=6 per genotype). **(C)** Immunofluorescence labeling of endogenous Fam172a in COS7 cells transfected with the pEYFP-ER plasmid (Clontech) and counterstained with DAPI (n=6). White arrowheads indicate ER localization. Scale bar, 200µm (A-B), 25µm (C).

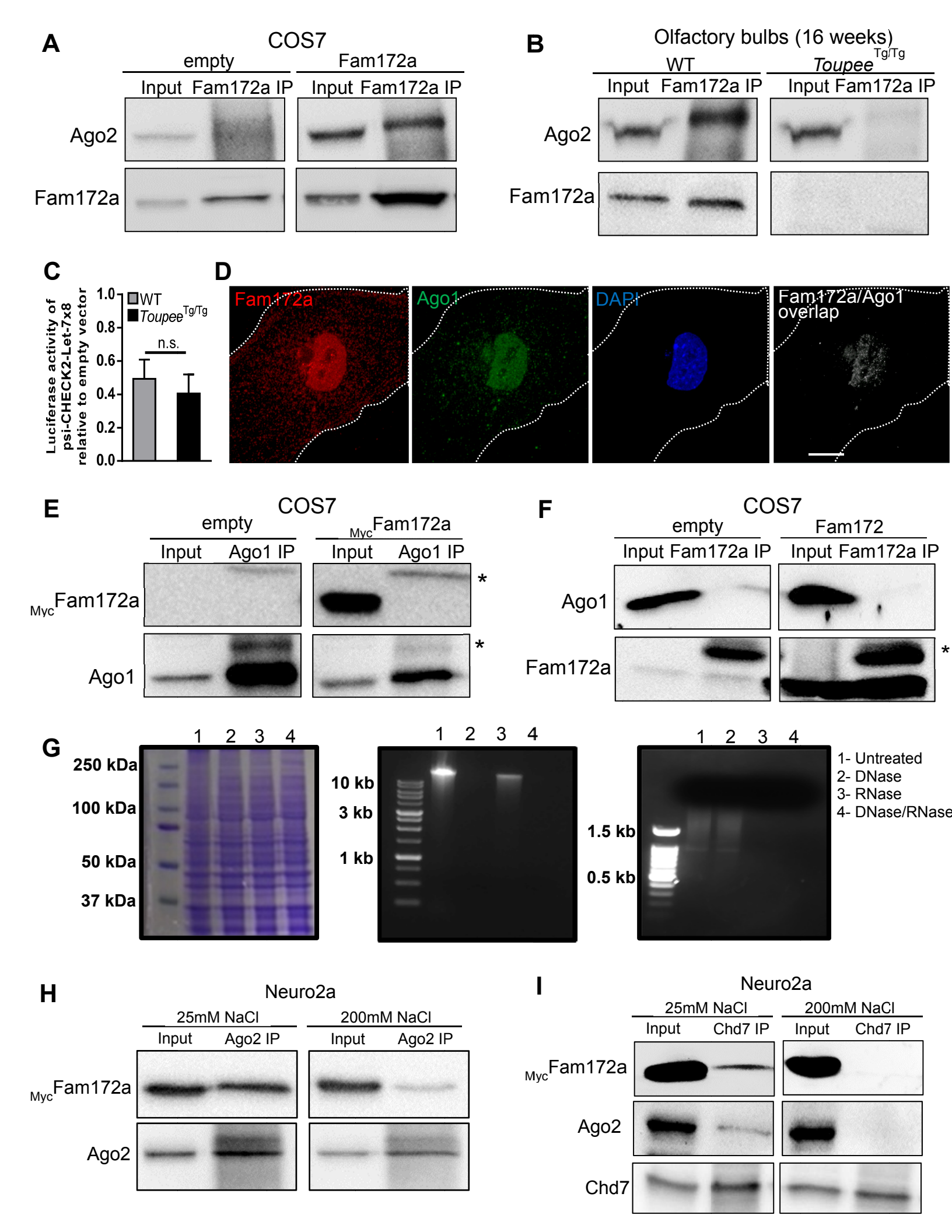
A
COS7
empty
Fam172a
Input Fam172a IP
Input Fam172a IP
Ago2
Fam172a
B
Olfactory bulbs (16 weeks)
WT
Toupee Tg/Tg
Input Fam172a IP
Input Fam172a IP
Ago2
Fam172a
C
Luciferase activity of psi-CHECK2-Let-7x8 relative to empty vector
1.0
0.8
0.6
0.4
0.2
0.0
WT
Toupee Tg/Tg
n.s.
D
Fam172a
Ago1
DAPI
Fam172a/Ago1 overlap
E
COS7
empty
Myc Fam172a
Input Ago1 IP
Input Ago1 IP
Myc Fam172a
Ago1
*
*
F
COS7
empty
Fam172
Input Fam172a IP
Input Fam172a IP
Ago1
Fam172a
*
G
1 2 3 4
250 kDa
100 kDa
50 kDa
37 kDa
1 2 3 4
10 kb
3 kb
1 kb
1 2 3 4
1.5 kb
0.5 kb
1- Untreated
2- DNase
3- RNase
4- DNase/RNase
H
Neuro2a
25mM NaCl
200mM NaCl
Input Ago2 IP
Input Ago2 IP
Myc Fam172a
Ago2
I
Neuro2a
25mM NaCl
200mM NaCl
Input Chd7 IP
Input Chd7 IP
Myc Fam172a
Ago2
Chd7

Figure S8. Fam172a physically interacts with Ago2 but not with Ago1. (A-B) Co-IP assays using whole cell extracts of COS7 cells (A; transfected with a Fam172a-expressing or empty vector) or of adult mouse olfactory bulbs (B; WT *vs* *Toupee*$^{Tg/Tg}$). IPs were performed with an anti-Fam172a antibody and analyzed by western blot using an anti-Ago2 antibody. Inputs correspond to 10% of protein extracts used for IP (n=3 per condition). **(C)** Luciferase activity from the psi-CHECK2-let-7x8 reporter relative to empty psi-CHECK2 vector in cultures of dissociated e10.5 embryos (WT *vs* *Toupee*$^{Tg/Tg}$). **(D)** Double immunofluorescence labeling of Fam172a (red) and Ago1 (green) in dissociated cells from WT e10.5 embryos (n=7). DAPI was used to counterstain nuclei (blue). The right panel shows the overlap of Fam172a and Ago1 signals (Pearson's correlation coefficient of 0.63) as determined with the AutoQuant 3X software. Scale bar: 25µm. **(E-F)** Co-IP assays using whole cell extracts of COS7 cells transfected with empty or $_{Myc}$Fam172a-expressing vector. IPs were performed with an anti-Ago1 (E) or anti-Fam172a (F) antibody and analyzed by western blot using anti-Ago1 and either anti-Myc (E) or anti-Fam172a (F) antibodies. Inputs correspond to 10% of protein extracts used for IP (n=3 per condition). The asterisk indicates the presence of mouse IgG heavy chain. **(G)** Impact of DNase and RNase treatments on the integrity of proteins (left panel), DNA (middle panel) and RNA (right panel) in whole-cell extracts, as described in Fig.4B. **(H-I)** Co-IP assays using whole cell extracts of Neuro2A cells (transfected with a $_{Myc}$Fam172a-expressing vector) in presence of different concentrations of NaCl. IPs were performed with an anti-Ago2 (H) or anti-Chd7 (I) antibody and analyzed by western blot using anti-Myc, anti-Ago2 and anti-Chd7 antibodies. Inputs correspond to 10% of protein extracts used for IP (n=3 per condition).

Figure S9

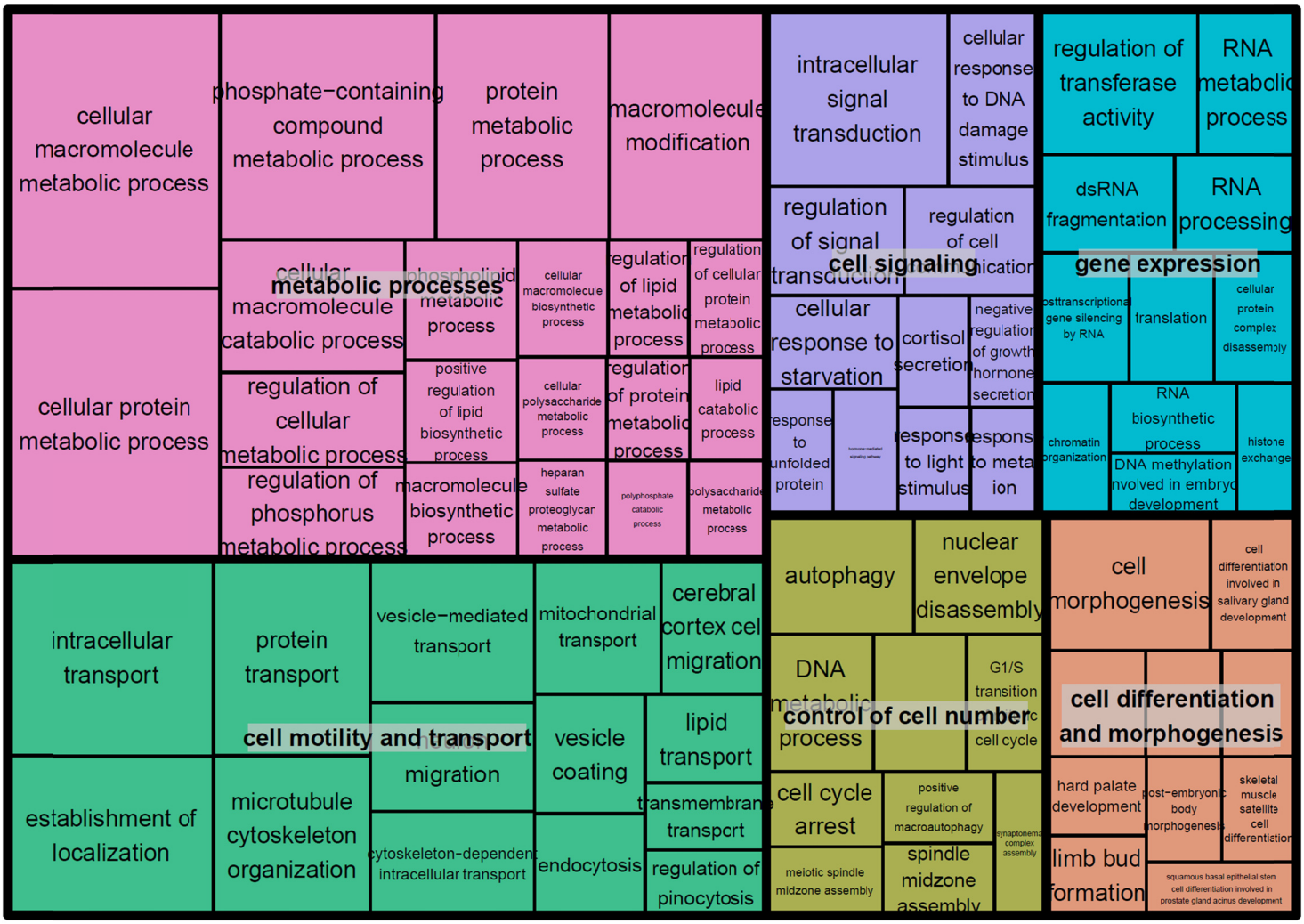

Figure S9. Enriched GO terms associated with the modulated transcript variants in *Toupee*$^{Tg/Tg}$ NCCs. REVIGO TreeMap representation of the GO analysis of the 1166 aberrantly spliced transcripts displayed in Fig.4C. The 75 enriched terms (ontology level ≥ 5 and $P < 0.05$) are distributed into 6 main categories: Metabolic processes; Cell motility and transport; Cell signaling; Gene expression; Control of cell number; and Cell differentiation and morphogenesis. Size of boxes is proportional to statistical significance.

Figure S10

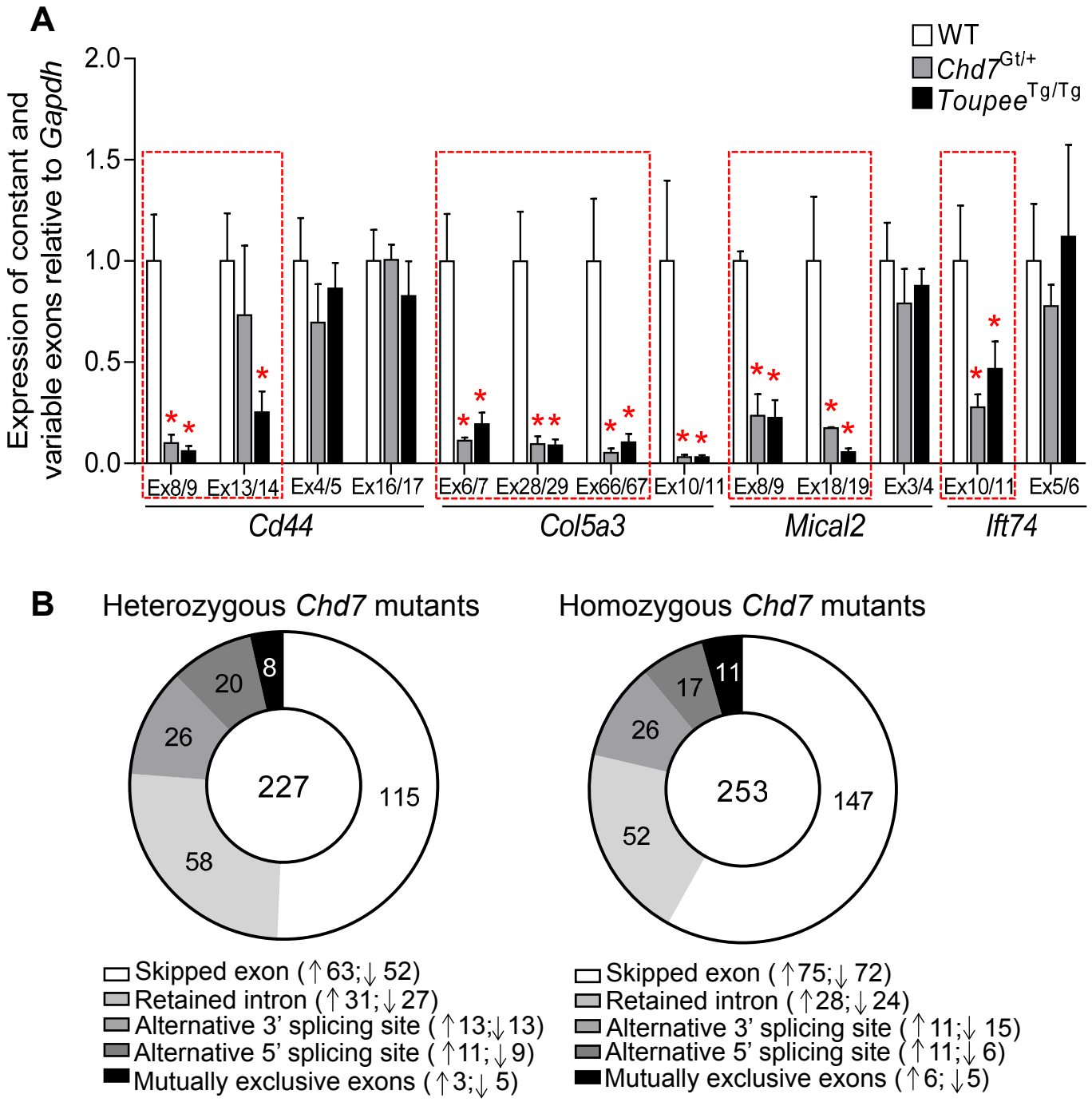

Figure S10. Detailed analysis of alternative splicing in *Toupee*$^{Tg/Tg}$ and *Chd7*$^{Gt/+}$ mutants. (A) RT-qPCR analysis of variably (delineated in red) and constantly expressed regions of 4 previously described Ago2-regulated genes (*Cd44*, *Col5a3*, *Mical2* and *Ift74*) in the head of *G4-RFP* (WT), *Toupee*$^{Tg/Tg}$*;G4-RFP* (*Toupee*$^{Tg/Tg}$) and *Chd7*$^{Gt/+}$ e12.5 embryos (n=5 per genotype). Transcript levels were normalized relative to *Gapdh*. * $P \leq 0.05$ (Student's *t*-test). **(B)** Donut chart showing the distribution of the differentially modulated alternative splicing events ($P<0.05$; variation in inclusion level ≥ 0.1) in P7 granule neuron progenitors from heterozygous (227 events; Dataset S3) and homozygous (253 events; Dataset S4) *Chd7* mutants as determined by rMATS-based analysis of recently published RNAseq data (22). Upward- and downward-pointing arrows indicate splicing events that are over- and under-represented in *Chd7* mutants, respectively.

Figure S11

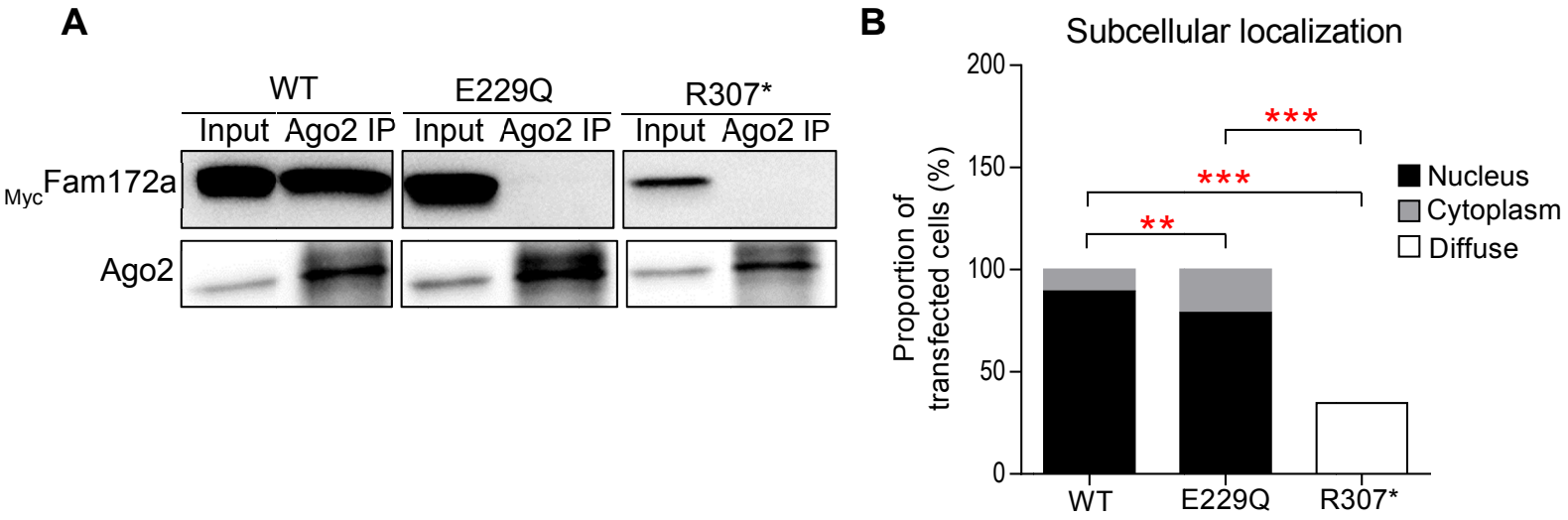

Figure S11: Variants of Fam172 identified in human CHARGE patients fail to interact with Ago2. **(A)** Co-IP assays using whole cell extracts of Neuro2A cells transfected with $_{Myc}$Fam172a-, $_{Myc}$Fam172a^{E229Q}- or $_{Myc}$Fam172a^{R307*}-expressing plasmids. Following Ago2 IP, the presence of Myc-tagged Fam172a and Ago2 proteins was revealed using anti-Myc and anti-Ago2 antibodies, respectively. Inputs correspond to 10% of protein extracts used for IP (n=3 per condition). **(B)** Quantification of Fam172a localization following anti-Myc immunofluorescence labeling of Neuro2A cells transfected with $_{Myc}$Fam172a, $_{Myc}$Fam172a^{E229Q} or $_{Myc}$Fam172a^{R307*} expression vectors. ** $P \leq 0.01$, *** $P \leq 0.001$ (Student's *t*-test)

Figure S12

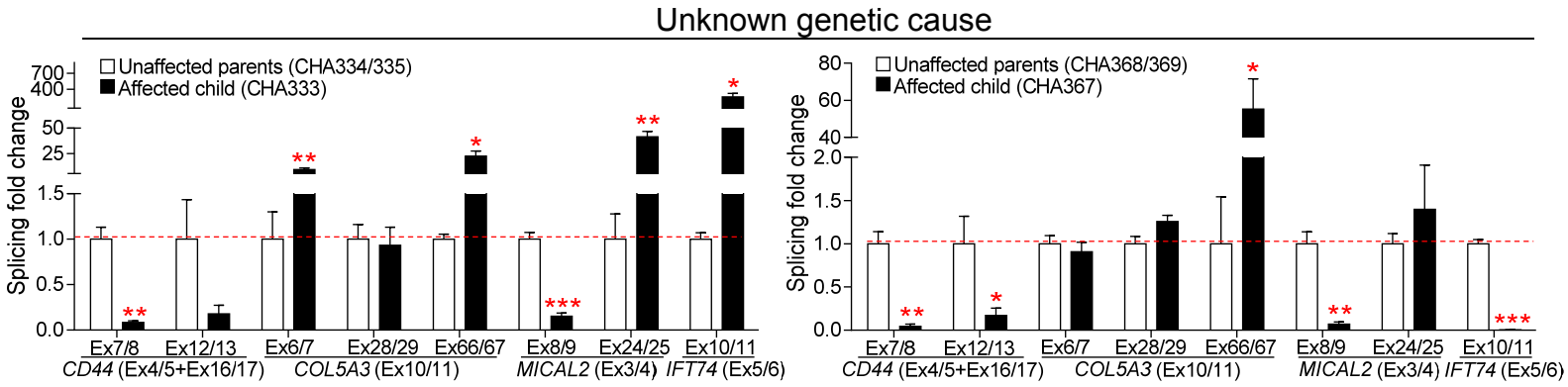

Figure S12: Dysregulation of alternative splicing in supplemental CHARGE syndrome patients. RT-qPCR analysis of splicing events for *CD44*, *COL5A3*, *MICAL2* and *IFT74* in lymphoblastoid cell lines. Expression levels of variable regions were normalized with levels of corresponding constant regions (indicated between parentheses). Results for unaffected parents were combined and used as reference value for calculation of splicing fold change (red dashed line). Each graph depicts the results obtained for a given family (for each individual, n=9 from 3 independent experiments). Results for other families can be found in Fig.5A-C, while detailed information about each patient can be found in Table S8. * $P \leq 0.05$, ** $P \leq 0.01$, *** $P \leq 0.001$ (Student's *t*-test).

Figure S13

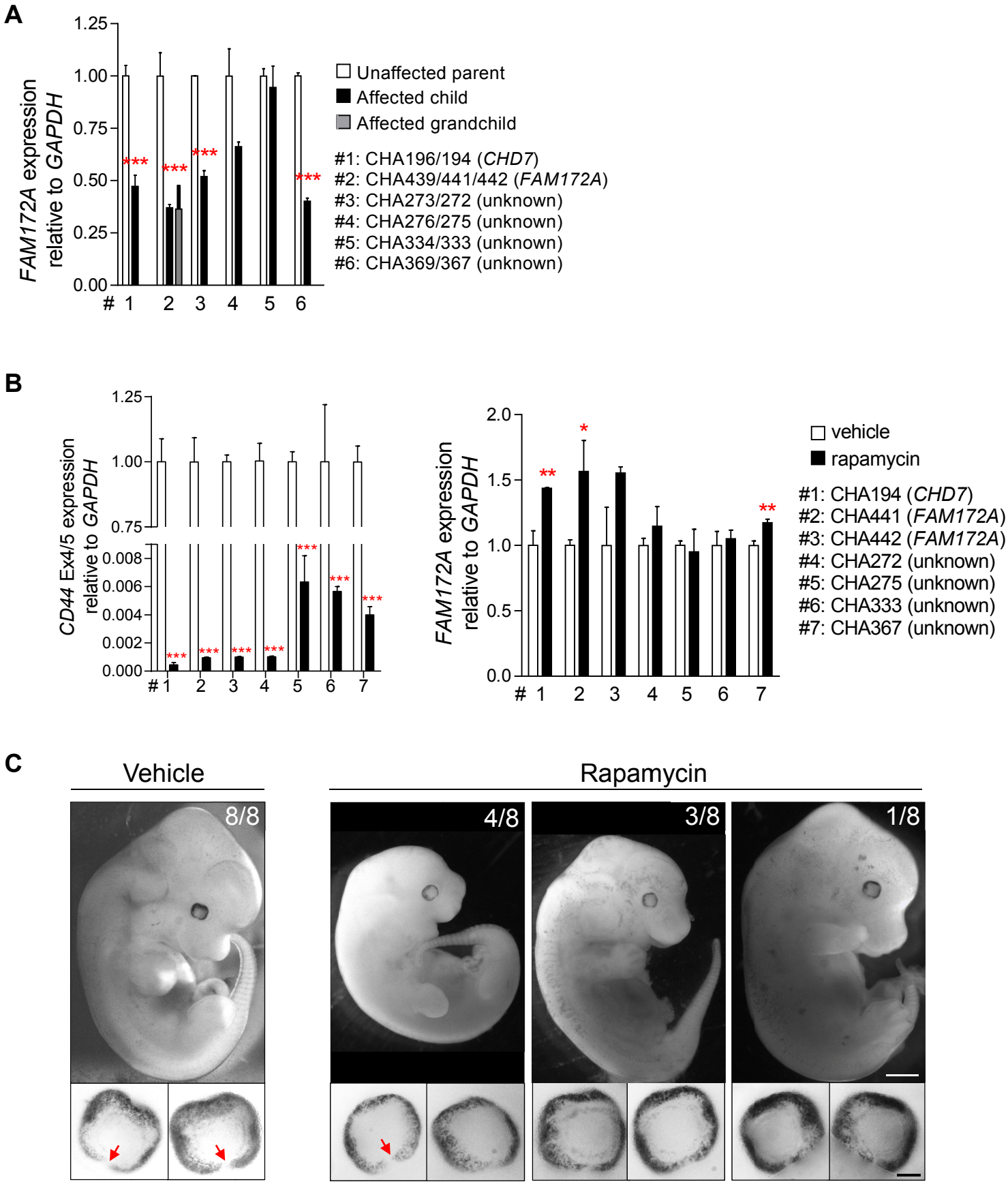
A
FAM172A expression relative to GAPDH
1.25
1.00
0.75
0.50
0.25
0.00
1 2 3 4 5 6
Unaffected parent
Affected child
Affected grandchild
#1: CHA196/194 (CHD7)
#2: CHA439/441/442 (FAM172A)
#3: CHA273/272 (unknown)
#4: CHA276/275 (unknown)
#5: CHA334/333 (unknown)
#6: CHA369/367 (unknown)
B
CD44 Ex4/5 expression relative to GAPDH
1.25
1.00
0.75
0.008
0.006
0.004
0.002
0.000
1 2 3 4 5 6 7
FAM172A expression relative to GAPDH
2.0
1.5
1.0
0.5
0.0
1 2 3 4 5 6 7
vehicle
rapamycin
#1: CHA194 (CHD7)
#2: CHA441 (FAM172A)
#3: CHA442 (FAM172A)
#4: CHA272 (unknown)
#5: CHA275 (unknown)
#6: CHA333 (unknown)
#7: CHA367 (unknown)
C
Vehicle
Rapamycin
8/8
4/8
3/8
1/8

Figure S13: Analysis of rapamycin effects in human LCLs and *Toupee*$^{Tg/Tg}$ mouse embryos. (A-B) *GAPDH*-normalized RT-qPCR analyses of *FAM172A* and *CD44* expression in human LCLs derived from CHARGE patients and/or one of their unaffected parents, in absence (A) or presence (B) of rapamycin. The decreased expression of *CD44* constant exons 4-5 demonstrates the efficacy of the rapamycin treatment (left panel in B). Note that basal expression of *FAM172A* is generally lower in CHARGE patients and that rapamycin has very little effect on it (right panel in B). **(C)** Bright field images of e12.5 *Toupee*$^{Tg/Tg}$ embryos that were previously exposed to vehicle (20% ethanol) or rapamycin (1mg/kg) for 3 days *in utero* (n=8 embryos per condition). Exposition to rapamycin decreased the incidence of coloboma (red arrows in bottom panels), while it also increased the incidence of growth retardation and malformation/resorption. The ratios displayed in the top right corner of top panels refer to the number of embryos with similar morphology, which is not correlated with their ocular phenotype. Scale bar, 1mm (whole embryos) or 50µm (eyes).

Figure S14

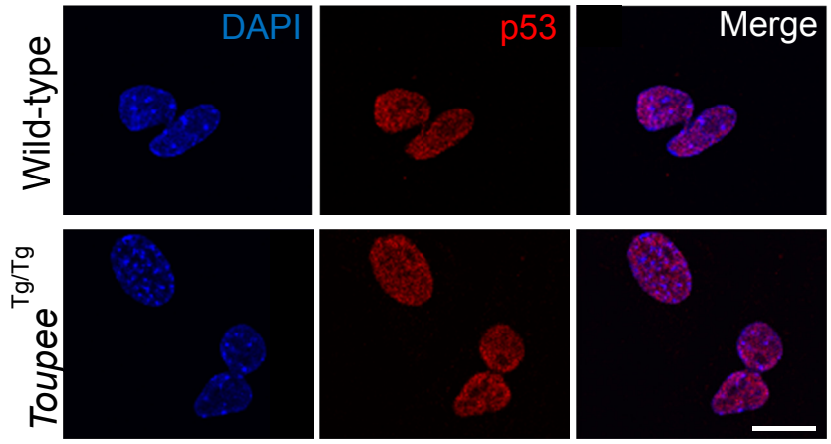

Figure S14: p53 expression appears unaffected in *Toupee*$^{Tg/Tg}$ embryos. Immunofluorescence analysis of p53 protein distribution in dissociated cells from WT and *Toupee*$^{Tg/Tg}$ e10.5 embryos. Neither the expression levels of p53 nor its localization appears affected in *Toupee*$^{Tg/Tg}$ cells. Scale bar, 10μm

Table S1: Overview of major and minor features of CHARGE syndrome in *Toupee*$^{Tg/Tg}$ mice

	Abnormality		Frequency
Major	Coloboma of the eye		86% (n=14)[a]
	Inner ear defects (circling behavior)		67% (n=61)
	Cleft palate		21% (n=14)
Minor	Heart malformation (left ventricular hypertrophy)		80% (n=10)
	Cranial nerve anomalies (VII, IX and/or X)		60% (n=10)
	Retardation of growth		61% (n=61)
	Genital abnormalities	Males (cryptorchidism)	52% (n=27)
		Females (hypoplastic uterine horns)	58% (n=12)
	Thymus hypoplasia		36% (n=22)
	Olfactory bulb hypoplasia		30% (n=10)
	Craniofacial malformations	Delayed closure of fontanelles	30% (n=10)
		Twisted skull	18% (n=61)
		Oropharyngeal atresia	16% (n=61)
	Kidney hypoplasia		8% (n=12)

Note: [a]10/14 unilateral, 2/14 bilateral.

Table S2: *Toupee*$^{Tg/Tg}$ mice are subfertile

Reproduction parameter	WT males WT females (n = 9 couples)	*Toupee*$^{Tg/Tg}$ males WT females (n = 10 couples)	WT males *Toupee*$^{Tg/Tg}$ females (n = 9 couples)
Average number of days before vaginal plug	1.33 ± 1.00	1.92 ± 0.79$^{n.s.}$	7.73 ± 6.60*
Average number of pups per litter	11.11 ± 1.76	7.44 ± 2.92**	7.00 ± 0.66*
Number of unproductive matings	0	1	5

Note: n.s. not significant; *P<0.05; **P<0.01.

Table S3: Genetic interaction between *Toupee*^{Tg} and *Chd7*^{Gt} alleles

Genotype / Phenotype	*Chd7*$^{Gt/+}$ (n=29) [a]	*Toupee*$^{Tg/+}$ (n=32) [b]	*Toupee*$^{Tg/+}$;*Chd7*$^{Gt/+}$ (n=20) [b]
Frequency at birth (expected)	49% (50%)	62% (50%)	38% (50%)
Weight at P25 (g)	11.40 ± 2.01	13.26 ± 2.14	6.69 ± 2.56
Premature postnatal death (≤P30)	3%	0%	20%
Circling behavior	27%	0%	45%
Male-to-female sex reversal (number of XY)	12% (16)	0% (15)	33% (12)
Width of choroidal fissure at e12.5 (μm) [c]	10.32 ± 8.16	4.23 ± 7.40	26.37 ± 27.31

Note: [a] From *Chd7*$^{Gt/+}$ X WT FVB/N crosses
[b] From *Chd7*$^{Gt/+}$ X *Toupee*$^{Tg/Tg}$ crosses
[c] n=16 for *Chd7*$^{Gt/+}$ and 34 for the others

Table S4: Dysregulation of the NCC gene regulatory network in *Toupee*$^{Tg/Tg}$ NCCs

Category	Gene name
Effectors of neural crest induction signals	*Lef1, Lrp5, Fzd3, Fzd5*, Fzd7, Bmpr1a, Bmpr2, Smad1, Smad5, Notch1,Notch2, Notch3, Dll1, Hes5*
Neural crest specifiers	*Sox8, Sox10, Tfap2a, Tfap2b, Tfap2c, Pax3, Mycn, Meis3, Dnmt3a, Dnmt3b, Ets1, Cited4*, Nr2f2, Tead1, Tead2*
Neural crest AP patterning	*Ednra, Hoxb2, Hoxa3, Hoxb5*
Neural crest EMT and migration	*Lims1*, Cdh2, Cdh6, Mmp14, Adam10*, Rxrg, Gja1, Vangl1*, Vangl2, Prickle1, Prickle2, Daam2, Ptk7, Celsr1, Celsr2, Celsr3, Erbb2, Erbb3, Erbb4*
Neural crest pathfinding	*Ephb3, Epha7, Ephb2, Ephb4, Epha8*, Efna5, Nrp1, Nrp2, Plxna1, Plxna3, Plxna4, Plxnb1, Plxnc1, Sema3b, Sema3d, Sema3g, Sema4c, Sema4g, Sema6a, Robo1, Robo2, Slit2, Slit3*
Craniofacial differentiation	*Sox5, Alx3, Rara*
Melanocyte differentiation	*Mitf , Tyr, Dct, Mef2c, Kit, Nf1, Ctbp2*
Neuronal differentiation	*Phox2b, Phox2a, Hand2, Ascl1, Th, Dbh, Runx1**
Glial differentiation	*Plp1, Fabp7, Rela**
Enteric nervous system	*Ednrb, Ret, Gfra1, Gfra2, Gfra3, Foxo3*, L1cam, Dcc, Kif26a, Lgi4, Prokr1**

Note: Genes included were those whose expression was modulated at least 1.5-fold ($P \leq 0.01$). Asterisks indicate upregulated genes.

Table S5: Fam172a interacting proteins in the chromatin fraction of Neuro2a cells

Category	Protein name	Gene name	Accession number	MW (kDa)	emPAI
Histones	Histone H4	Hist1h4a	P62806	11	**10,000**
	Histone H3.2	Hist1h3b	P84228	15	**5,640**
	Histone H2A type 2-A	Hist2h2aa1	Q6GSS7	14	**5,143**
	Core histone macro-H2A.1	H2afy	Q9QZQ8	39	**2,480**
	Histone H2AX	H2afx	P27661	15	**1,577**
	Histone H1.5	Hist1h1b	P43276	22	**1,415**
	Histone H1.1	Hist1h1a	P43275	21	**1,167**
	Histone H1.3	Hist1h1d	P43277	22	**0,716**
	Histone H1.2	Hist1h1c	P15864	21	**0,673**
	Histone H1.4	Hist1h1e	P43274	21	**0,598**
	H1 histone family, member X	H1fx	Q80ZM5	20	**0,149**
	Histone H1.0	H1f0	P10922	20	**0,126**
Histone regulators	Histone-binding protein RBBP7	Rbbp7	Q60973	47	**0,138**
	Histone-lysine N-methyltransferase ASH1L	Ash1l	Q99MY8	331	**0,082**
	Histone deacetylase 2	Hdac2	P70288	55	**0,068**
	Histone deacetylase 7	Hdac7	Q8C2B3	101	**0,046**
	Histone-lysine N-methyltransferase EHMT2	Ehmt2	Q9Z148	138	**0,013**
	JmjC domain-containing histone demethylation protein 2C	Jmjd1c	Q69ZK6	260	**0,003**
Other chromatin factors	Regulator of chromosome condensation	Rcc1	Q8VE37	44	**0,374**
	FACT complex subunit SSRP1	Ssrp1	Q08943	81	**0,137**
	Heterochromatin protein 1-binding protein 3	Hp1bp3	Q3TEA8	60	**0,013**
	DNA replication licensing factor MCM5	Mcm5	P49718	82	**0,009**
mRNA splicing	Serine/arginine-rich splicing factor 1	Srsf1	Q6PDM2	27	**1,410**
	Heterogeneous nuclear ribonucleoprotein A/B	Hnrnpab	Q99020	30	**0,796**
	Heterogeneous nuclear ribonucleoprotein K	Hnrnpk	P61979	50	**0,698**
	Heterogeneous nuclear ribonucleoprotein D0	Hnrnpd	Q60668	38	**0,314**
	Heterogeneous nuclear ribonucleoproteins C1/C2	Hnrnpc	Q9Z204	34	**0,303**
	Polypyrimidine tract-binding protein 1	Ptbp1	P17225	56	**0,183**
	Serine/arginine-rich splicing factor 7	Srsf7	Q8BL97	30	**0,083**
	ELAV-like protein 1	Elavl1	P70372	36	**0,075**
	NHP2-like protein 1	Nhp2l1	E9PZS4	5	**0,055**
	RNA-binding protein FUS	Fus	P56959	52	**0,048**
	Intron-binding protein aquarius	Aqr	Q8CFQ3	170	**0,011**
RNA processing	Ribosomal L1 domain-containing protein 1	Rsl1d1	Q8BVY0	50	**0,242**
	Pumilio domain-containing protein KIAA0020	Kiaa0020	Q8BKS9	72	**0,051**
	U3 small nucleolar RNA-associated protein 18 homolog	Utp18	Q5SSI6	61	**0,012**
Ribosome biogenesis	40S ribosomal protein S3	Rps3	P62908	26	**2,542**
	Nucleophosmin	Npm1	Q61937	32	**2,540**
	Nucleolin	Ncl	P09405	76	**0,975**
	60S ribosomal protein L18a	Rpl18a	P62717	20	**0,700**
	60S ribosomal protein L5	Rpl5	P47962	34	**0,325**
	60S ribosomal protein L6	Rpl6	P47911	33	**0,311**
	Nucleolar transcription factor 1	Ubtf	P25976	89	**0,132**
	40S ribosomal protein S25	Rps25	P62852	13	**0,129**
	60S ribosomal protein L22	Rpl22	P67984	14	**0,053**
	60S ribosomal protein L19	Rpl19	P84099	23	**0,033**
GTPase-related proteins	GTP-binding nuclear protein Ran	Ran	P62827	24	**0,430**
	GTP-binding protein Di-Ras2	Diras2	Q5PR73	22	**0,076**
	Arf-GAP with SH3 domain, ANK repeat and PH domain-containing protein 2	Asap2	Q7SIG6	106	**0,016**

Cytoskeleton-associated proteins	Actin, cytoplasmic 1	Actb	P60710	41	**1,141**
	Neuronal migration protein doublecortin	Dcx	O88809	40	**0,256**
	Junction plakoglobin	Jup	Q02257	81	**0,155**
	Echinoderm microtubule-associated protein-like 6	Eml6	Q5SQM0	217	**0,008**
	Desmoglein-1-alpha	Dsg1a	Q61495	114	**0,007**
Other	Casein kinase II subunit alpha	Csnk2a1	Q60737	45	**0,247**
	Elongation factor 1-alpha 1	Eef1a1	P10126	50	**0,087**
	Glyceraldehyde-3-phosphate dehydrogenase	Gapdh	P16858	35	**0,095**
	Chymotrypsinogen B	Ctrb1	Q9CR35	27	**0,062**
	Voltage-dependent anion-selective channel protein 3	Vdac3	Q60931	30	**0,053**
	Sorting nexin-29	Snx29	Q9D3S3	91	**0,031**
	Stress-70 protein, mitochondrial	Hspa9	P38647	73	**0,021**
	Fibrous sheath-interacting protein 2	Fsip2	A2ARZ3	784	**0,019**

Note: Proteins were included if enriched at least 1.5-fold in comparison to the MBP negative control and detected in at least two out of the three biological replicates of this analysis. The indicated emPAI (exponentially modified Protein Abundance Index) value corresponds to the average of the three biological replicates. Accession number is for the Uniprot database.

Table S6: Fam172a interacting proteins in the nucleoplasm fraction of Neuro2a cells

Category	Protein name	Gene name	Accesion number	MW	emPAI
RNA binding /processing	Lupus La protein homolog	Ssb	P32067	47	**0,217**
	ATP-dependent RNA helicase A	Dhx9	O70133	149	**0,090**
	Nucleoprotein TPR	Tpr	F6ZDS4	273	**0,053**
	Exosome complex component MTR3	Exosc6	Q8BTW3	28	**0,039**
	tRNA (cytosine(34)-C(5))-methyltransferase	Nsun2	Q1HFZ0	85	**0,030**
	DAZ-associated protein 1	Dazap1	Q9JII5	43	**0,025**
	Heterogeneous nuclear ribonucleoprotein Q	Syncrip	Q7TMK9	69	**0,016**
	Bifunctional glutamate/proline--tRNA ligase	Eprs	Q8CGC7	170	**0,008**
mRNA splicing	Nuclease-sensitive element-binding protein 1	Ybx1	P62960	35	**0,130**
	Serine/arginine-rich splicing factor 3	Srsf3	P84104	19	**0,114**
	Pre-mRNA-splicing regulator WTAP	Wtap	Q9ER69	44	**0,084**
	Interleukin enhancer-binding factor 2	Ilf2	Q9CXY6	43	**0,080**
	TAR DNA-binding protein 43	Tardbp	Q921F2	44	**0,039**
	RNA-binding protein FUS	Fus	P56959	52	**0,021**
	Far upstream element-binding protein 2	Khsrp	Q3U0V1	76	**0,018**
DNA binding/repair	Histone-binding protein RBBP7	Rbbp7	Q60973	47	**0,173**
	Superoxide dismutase [Cu-Zn]	Sod1	P08228	15	**0,140**
	DNA damage-binding protein 1	Ddb1	Q3U1J4	126	**0,029**
	DNA dC->dU-editing enzyme APOBEC-3	Apobec3	Q99J72	50	**0,023**
	Tyrosine-protein kinase BAZ1B	Baz1b	Q9Z277	170	**0,018**
	Tumor suppressor p53-binding protein 1	Tp53bp1	P70399	211	**0,002**
Cytoskeleton-associated proteins	Tubulin beta-5 chain	Tubb5	P99024	49	**0,546**
	MARCKS-related protein	Marcksl1	P28667	20	**0,088**
	Peripherin	Prph	P15331	53	**0,083**
	WD repeat-containing protein 1	Wdr1	O88342	66	**0,064**
	Drebrin	Dbn1	Q9QXS6	77	**0,021**
	Echinoderm microtubule-associated protein-like 6	Eml6	Q5SQM0	217	**0,005**
	Spectrin beta chain, non-erythrocytic 1	Sptbn1	Q62261	274	**0,004**
	Microtubule-actin cross-linking factor 1	Macf1	Q9QXZ0	831	**0,001**
Other	Leukocyte elastase inhibitor B	Serpinb1b	Q8VHP7	42	**1,870**
	Elongation factor 1-alpha 1	Eef1a1	P10126	50	**0,360**
	ATP synthase subunit alpha	Atp5a1	Q03265	59	**0,299**
	GTP-binding protein Di-Ras2	Diras2	Q5PR73	22	**0,285**
	40S ribosomal protein S3	Rps3	P62908	26	**0,233**
	Malate dehydrogenase, mitochondrial	Mdh2	P08249	35	**0,165**
	Fibrous sheath-interacting protein 2	Fsip2	A2ARZ3	784	**0,110**
	Myristoylated alanine-rich C-kinase substrate	Marcks	P26645	29	**0,061**
	Asparagine synthetase	Asns	Q61024	64	**0,037**
	E3 ubiquitin-protein ligase TRIM8	Trim8	Q99PJ2	61	**0,019**
	Teneurin-1	Tenm1	Q9WTS4	305	**0,003**

Note: Proteins were included if enriched at least 1.5-fold in comparison to the MBP negative control and detected in at least two out of the three biological replicates of this analysis. The indicated emPAI (exponentially modified Protein Abundance Index) value corresponds to the average of the three biological replicates. Accession number is for the Uniprot database.

Table S7: Fam172a interacting proteins in the cytoplasm fraction of Neuro2a cells

Category	Protein name	Gene name	Accesion number	MW	emPAI
RNA binding /processing	Bifunctional glutamate/proline--tRNA ligase	Eprs	Q8CGC7	170	**0,259**
	Nuclease-sensitive element-binding protein 1	Ybx1	P62960	36	**0,148**
	Eukaryotic translation initiation factor 2 subunit 1	Eif2s1	Q6ZWX6	36	**0,039**
	RNA-binding protein FUS	Fus	P56959	52	**0,015**
	Squamous cell carcinoma antigen recognized by T-cells 3	Sart3	Q9JLI8	109	**0,007**
Nucleotide binding /processing	ATP synthase subunit beta, mitochondrial	Atp5b	P56480	56	**1,565**
	ADP/ATP translocase 1	Slc25a4	P48962	32	**1,384**
	Nucleoside diphosphate kinase A	Nme1	P15532	17	**1,307**
	High mobility group protein B2	Hmgb2	P30681	24	**0,523**
	ADP/ATP translocase 2	Slc25a5	P51881	286	**0,518**
	Up-regulated during skeletal muscle growth protein 5	Usmg5	Q78IK2	5	**0,410**
	ATP synthase subunit gamma, mitochondrial	Atp5c1	Q91VR2	32	**0,126**
	GTP-binding protein Di-Ras2	Diras2	Q5PR73	22	**0,074**
	5'-AMP-activated protein kinase catalytic subunit alpha-1	Prkaa1	Q5EG47	63	**0,048**
	Arf-GAP with SH3 domain, ANK repeat and PH domain-containing protein 2	Asap2	Q7SIG6	106	**0,015**
Protein processing /repair	Peptidyl-prolyl cis-trans isomerase A	Ppia	P17742	17	**6,238**
	Prohibitin	Phb	P67778	29	**2,208**
	Elongation factor 1-alpha 1	Eef1a1	P10126	50	**1,083**
	Prohibitin-2	Phb2	O35129	33	**0,825**
	Elongation factor 2	Eef2	P58252	95	**0,624**
	Elongation factor 1-gamma	Eef1g	Q9D8N0	44	**0,465**
	T-complex protein 1 subunit alpha	Tcp1	P11983	60	**0,345**
	Aminoacyl tRNA synthase complex-interacting multifunctional protein 2	Aimp2	Q8R010	35	**0,249**
	Thioredoxin	Txn	P10639	11	**0,238**
	Prolyl endopeptidase	Prep	Q9QUR6	80	**0,191**
	26S protease regulatory subunit 6B	Psmc4	P43686	47	**0,058**
	Transcription factor BTF3	Btf3	Q64152	22	**0,057**
	Alpha-2-HS-glycoprotein	Ahsg	P29699	37	**0,028**
Metabolic processes	Glyceraldehyde-3-phosphate dehydrogenase	Gapdh	P16858	35	**1,586**
	L-lactate dehydrogenase A chain	Ldha	P06151	36	**1,005**
	Aspartate aminotransferase, mitochondrial	Got2	P05202	47	**0,767**
	Glucose-6-phosphate isomerase	Gpi	P06745	62	**0,412**
	Bifunctional purine biosynthesis protein PURH	Atic	Q9CWJ9	65	**0,298**
	D-3-phosphoglycerate dehydrogenase	Phgdh	Q61753	56	**0,290**
	Fatty acid-binding protein, epidermal	Fabp5	Q05816	15	**0,255**
	Malate dehydrogenase, cytoplasmic	Mdh1	P14152	36	**0,190**
	Inorganic pyrophosphatase	Ppa1	Q9D819	32	**0,185**
	Cytosolic acyl coenzyme A thioester hydrolase	Acot7	Q91V12	42	**0,164**
	Dolichyl-diphosphooligosaccharide--protein glycosyltransferase	Ddost	O54734	49	**0,115**
	Dihydrolipoyllysine-residue succinyltransferase	Dlst	Q9D2G2	48	**0,086**
	Glycogen phosphorylase, brain form	Pygb	Q8CI94	96	**0,027**
	Procollagen-lysine,2-oxoglutarate 5-dioxygenase 3	Plod3	Q9R0E1	84	**0,025**
Cytoskeleton-associated proteins	Clathrin heavy chain 1	Cltc	Q68FD5	191	**0,220**
	T-complex protein 1 subunit gamma	Cct3	P80318	60	**0,197**
	Spectrin beta chain, non-erythrocytic 1	Sptbn1	Q62261	275	**0,065**
	Desmoplakin	Dsp	E9Q557	332	**0,046**

Other	Leukocyte elastase inhibitor B	Serpinb1b	Q8VHP7	42	**4,340**
	14-3-3 protein zeta/delta	Ywhaz	P63101	27	**1,015**
	Voltage-dependent anion-selective channel protein 1	Vdac1	Q60932	32	**0,519**
	Macrophage migration inhibitory factor	Mif	P34884	15	**0,480**
	Voltage-dependent anion-selective channel protein 3	Vdac3	Q60931	30	**0,306**
	Voltage-dependent anion-selective channel protein 2	Vdac2	Q60930	31	**0,113**

Note: Proteins were included if enriched at least 1.5-fold in comparison to the MBP negative control and detected in at least two out of the three biological replicates of this analysis. The indicated emPAI (exponentially modified Protein Abundance Index) value corresponds to the average of the three biological replicates. Accession number is for the Uniprot database.

Table S8: Genetic and phenotypic information about the CHARGE syndrome patients included in this study

Patient ID (sex)	*CHD7* variant	*FAM172A* variant	Possible transmission	Phenotypic presentation
CHA194 (XX female)	NM_017780.3: c.5050+1G>T	no	*De novo* dominant	Coloboma, choanal atresia, ear malformations, hearing loss, delayed puberty, short stature
CHA272 (XY male)	no	no	Recessive or *de novo* dominant	Coloboma, choanal atresia, ear malformation, hearing loss, heart malformation, swallowing problems, developmental delay
CHA275 (XX female)	no	no	Recessive or *de novo* dominant	Choanal atresia, Mondini malformation, hearing loss, growth retardation, swallowing problems
CHA333 (XX female)	no	no	Recessive or *de novo* dominant	Coloboma, choanal stenosis, hearing loss, ear malformation, heart malformation, short stature, swallowing problems
CHA367 (XX female)	no	no	Recessive or *de novo* dominant	Coloboma, hypoplastic optic nerves, unilateral choanal atresia, ear malformation, heart malformation, short stature, agenesis of corpus callosum, swallowing problems
CHA441[a] (XX female)	no	NM_032042.5: c.682G>C	*De novo* dominant	Choanal atresia, small abnormal ears, moderate hearing loss, vestibular dysfunction
CHA442[a] (XX female)	no	NM_032042.5: c.682G>C NM_032042.5: c.916C>T	Inherited from mother / *De novo* dominant	Choanal atresia, profound hearing loss, small left kidney, genital hypoplasia, delayed puberty, growth retardation, growth hormone deficiency, hypothyroidism

Note: [a] Mother (CHA441) and child (CHA442) from the same family.

Table S9: Genetic and phenotypic information about the *FAM172A* mutation-positive mother-child pair from the replication cohort

Family member	*CHD7* variant	*FAM172A* variant	Possible transmission	CHARGE syndrome-related features
Mother	no	NM_032042.5: c.682G>C	*De novo* dominant	Choanal atresia, blocked tear ducts, severe hearing loss, growth hormone deficiency hydronephrotic left kidney, hypothyroidism
Child	no	NM_032042.5: c.682G>C	Inherited from mother	Choanal atresia, blocked tear ducts, strabismus, abnormal ears, severe hearing loss, developmental delay, immune deficiency, hypothyroidism

Table S10: Antibodies used in this study

	Antibody Name	Dilution	Source	RRID
Primary Antibodies	Rabbit molyclonal Anti-Fam172a	WB (1:1000) IF (1:500) IP (2 µg/ml)	Abcam ab121364	AB_11127114
	Rat monoclonal Anti-AGO2	IF(1:1000)	Sigma SAB4200085	AB_10600719
	Rat monoclonal Anti-AGO1	WB (1:1000) IF (1:1000) IP (3 µg/ml)	Sigma SAB4200084	AB_10602786
	Rabbit monoclonal Anti-CHD7 (D3F5)	WB (1:1000) IP (3 µg/ml)	Cell Signaling #6505	AB_11220431
	Rabbit polyclonal Anti-AGO2	WB (1:1000) IF (1:500) IP (3 µg/ml)	Abcam ab32381	AB_867543
	Rabbit polyclonal Anti-Active Caspase 3	IF (1:500)	Abcam ab13847	AB_443014
	Goat polyclonal Anti-Sox10	IF (1:250)	Santa Cruz Sc-17342	AB_2195374
	Mouse monoclonal Anti-Neurofilament	IHC (1:500)	DSHB 2H3	AB_2618380
	Rabbit polyclonal Anti-H3	WB (1:2500) IP (1 µg/ml)	Abcam ab1791	AB_302613
	Rabbit polyclonal Anti-Ki67	IF (1:1000)	Abcam ab15580	AB_443209
	Mouse monoclonal Anti-p53	IF (1:250)	Cell Signaling #2524 (1C12)	AB_331743
	Mouse monoclonal Anti-Myc tag	WB (1:500) IF (1:100)	In house hybridoma (9E10)	-
Secondary Antibodies	Donkey Alexa Fluor 488 Anti-Rat IgG	IF (1:500)	Jackson ImmunoResearch 712-545-150	AB_2340683
	Donkey Alexa Fluor 594 Anti-Rabbit IgG	IF (1:500)	Jackson ImmunoResearch 711-585-152	AB_2340621
	Donkey Alexa Fluor 647 Anti-Mouse IgG	IF (1:500)	Jackson ImmunoResearch 715-605-150	AB_2340862
	Bovine Alexa Fluor 647 Anti-Goat IgG	IF (1:500)	Jackson ImmunoResearch 805-605-180	AB_2340885
	Donkey Anti-Rabbit IgG HRP	WB (1:10 000)	AbD Serotec Star124p	AB_615912
	Donkey Anti-Mouse IgG HRP	WB (1:10 000)	AbD Serotec Star117	AB_324488
	Goat Anti-Rat IgG HRP	WB (1:10 000)	Santa Cruz Sc-2032	AB_631755

Table S11: Oligonucleotide primers used for RT-qPCR

Oligo Name	Sequence (5'-3')
Fam172a Forward	AGG TGA CTG CTG TGG CAT TGA C
Fam172a Reverse	GGC TTC TGC GAG CTG CTC TT
FAM172A Forward	ACC GCC TCT TGA TTT TCC TGA
FAM172A Reverse	GCC TCG TAT CTT TTC TGG TTC C
Nr2f1 Forward	CTT TCA GGA ACA GGT GGA GAA GC
Nr2f1 Reverse	AGG AAC ACT GGA TGG ACA TGT AAG G
A830082K12Rik Forward	TTC AAT AGT TCT GCT GAA TGC TCC
A830082K12Rik Reverse	ATA AAG TAG GGA TCC GTT TCC AGT TGT GTC AAC
Pou5f2 Forward	AGT GTG GTT TTC TAA CCG GAG CCA
Pou5f2 Reverse	TCA GAG AAC TGA ACG CTA ACC CTG
Gapdh Forward	CTG TGG CGT GAT GGC CGT GG
Gapdh Reverse	CCT CAG TGT AGC CCA AGA TG
Cd44_Ex8 (v4) Forward	TAC CCC AGT TTT TCT GGA TCA GG
Cd44_Ex9 (v5) Reverse	GCC ATC CTG GTG GTT GTC TG
CD44_Ex7 (v4) Forward	AGG CTG GGA GCC AAA TGA AG
CD44_Ex8 (v5) Reverse	CCG GAT TTG AAT GGC TTG GG
Cd44_Ex13 (v9) Forward	TGG AAG ACT TGA ACA GGA CAG G
Cd44_Ex14 (v10) Reverse	GTT TTC GTC TTC TTC CGG CTC
CD44_Ex12 (v9) Forward	GCT TCA GCC TAC TGC AAA TCC
CD44_Ex13 (v10) Reverse	GCC TTC ATG TGA TGT AGA GAA GC
Cd44_Ex4 Forward	ACA GAC CTA CCC AAT TCC TTC G
_Ex5 Reverse	GGG TGC TCT TCT CGA TGG TG
CD44_Ex4 Forward	TGC CCA ATG CCT TTG ATG GAC
CD44_Ex5 Reverse	GAA GTG CTG CTC CTT TCA CTG
Cd44_Ex16 Forward	GGA GTT CCC GCA CTG TGA C
Cd44_Ex17 Reverse	GGT CTC CTC ATA GGA CCA GAA G
CD44_Ex16 Forward	AGG TGG AGC AAA CAC AAC CTC
CD44_Ex17 Reverse	GAA TCA AAG CCA AGG CCA AGA G
Col5a3_EX6 Forward	CCC CAA AGA CGA TGA ACC AG
Col5a3_EX7 Reverse	TCT CTG TCT CAG GGA TGT GGA
COL5A3_EX6 Forward	TCA AGT CCA CCT CCT GAC TCC
COL5A3_EX7 Reverse	TAG GAT CGT GGC ATT GAG TCC
Col5a3_EX28 Forward	TAC CTC TGG TAA CCG GGG TCT C
Col5a3_EX29 Reverse	CCT TTT GGT CCC TCA TCA CCC
COL5A3_EX28 Forward	AGG GGG AGA AAG GCG AGA A
COL5A3_EX29 Reverse	CCT TTT GGT CCC TCA TCA CCC
Col5a3_EX66 Forward	GCA GCC CAT CAG AGG TTC AC
Col5a3_EX67 Reverse	AAG AGG GTC TTC GCC TGT CC
COL5A3_EX66 Forward	ACC TAC TCC TGC CAG AAT GC

COL5A3_EX67 Reverse	GGT CTT CGT CTG TCC TTT CCG
Col5a3_EX10 Forward	GGA CAG CAG TTT GAG GGG
Col5a3_EX11 Reverse	CAC GGT CCC CAG GGA AG
COL5A3_EX10 Forward	GGG CAG CAG TTT GAG GGA C
COL5A3_EX11 Reverse	GGG TCG CCA GGG AAT CCT
Ift74_EX10 Forward	ACA CTT CAG CAA CAG CTA GAT TC
Ift74_EX11 Reverse	GGC GAT CCC ATG CTT TTG TC
IFT74_EX10 Forward	TCA ACA ACA ATT GGA TTC ACA GAA C
IFT74_EX11 Reverse	TGA TCT CGA TGG GAC TCC AAC
Ift74_EX5 Forward	TGT ACA ACC AAG AAA ATT CAG TGT
Ift74_EX6 Reverse	TGT TGT AGT CTG CTA GTT GTC CT
IFT74_EX5 Forward	TGT CAT ATG AAA AGA GGG CTG AG
IFT74_EX6 Reverse	TGT TGT AGT CTG CTA GTT GTC C
Mical2_EX8 Forward	GGA CAG TAC CCA CTA CTT TGT C
Mical2_EX9 Reverse	CCG AAC ACA GCA GCA TCT CT
MICAL2_EX8 Forward	CTG CTC GAC AAA GGT GTC ATC
MICAL2_EX9 Reverse	CGG GCA TAG GAT AGC AGG TT
Mical2_EX18 Forward	CGG GTC TCA GGC ATA GGT AAG
Mical2_EX19 Reverse	AGC CGG TAC TTG GTT GAG TTC
MICAL2_EX24 Forward	CGT GTG TAC GTG ATG GAA CG
MICAL2_EX25 Reverse	GCT TCA ACT CTG CCC GTC TC
Mical2_EX3 Forward	GTG GCA CAA ACT GGA TAA GCG
Mical2_EX4 Reverse	GCA GGA CAT TGT TCC GGG AG
MICAL2_EX3 Forward	CCT GGA AAG CCA AAG CCC TG
MICAL2_EX4 Reverse	GTT GTT CCG GGA GAA GGA GTC

Table S12: Oligonucleotide primers used for mouse genotyping as well as for cloning and mutagenesis of *Fam172a*

	Oligo Name	Sequence (5'-3')
Genotyping	Fam172a_Mut_Forward	GGG AGT AAG TCC TAC CAA TGT TAA ATC
	Fam172a_Mut_Reverse	TGA CCT TCT AAA CAG TCC CAT ATC CCC
	Fam172a_WT_Forward	GAA GTG GGA ACA AAA CAC CCT TGG
	Fam172a_WT_Reverse	CTA ATG AGT TTG GGG AAA TTA TCA TAG
	Chd7_WT/Mut_Forward	GCT CGC TTT TCA ACC TCA TTA CG
	Chd7_WT_Reverse	ATC AAC AAT GCC AAC CCA GGC
	Chd7_Mut_Reverse	CCT CCG ATT GAC TGA GTC GC
	Smcxy Forward	TGA AGC TTT TGG CTT TGA G
	Smcxy Reverse	CCA CTG CCA AAT TCT TTG G
	Zfy Forward	GAC CAG ATT GTT GTG GAA GTA CAA G
	Zfy Reverse	CCA GTG TGT CTG AAG TGT CAG CTG
Fam172a ORF and mutagenesis	*Fam172a* ORF (*Xho*I) Forward	CTC GAG ATG AAA AAG GAC GAA CCA CCT TTT GAT TTT CC
	Fam172a ORF*(Eco*RI) Reverse	GAA TTC TCA CAG CTC CTC GTG CTT GAT CC
	p.Glu229Gln (mut1_Arb2)	GGG AAG CGG **C**AA AGG AGA GAT AAG
	p.Arg307* (mut2_Arb2)	CTG ATG ATT CAA **T**GA GAA GCA GAT
	p.Ser294Ala (mut_hydrolase)	GTC CTC CAT AG**G** **C**AT GAG CCA CAA A

OTHER SUPPORTING INFORMATION

Dataset S1: RNAseq data of *Toupee*$^{Tg/Tg}$ NCCs analyzed with edgeR and DESeq (3488 genes; FC ≥ 1.5; DESeq $P \leq 0.01$).

Dataset S2: RNAseq data of *Toupee*$^{Tg/Tg}$ NCCs analyzed with rMATS (1166 events; inclusion level ≥ 0.1; $P < 0.01$) .

- **Sheet 1: Skipped exons (611 events)**
- **Sheet 2: Retained introns (368 events)**
- **Sheet 3: Alternative 3' splice site (91 events)**
- **Sheet 4: Alternative 5' splice site (69 events)**
- **Sheet 5: Mutually exclusive exons (27 events)**

Dataset S3: RNAseq data of *Chd7*-het granule neuron progenitors analyzed with rMATS (227 events; inclusion level ≥ 0.1; $P < 0.05$) .

- **Sheet 1: Skipped exons (115 events)**
- **Sheet 2: Retained introns (58 events)**
- **Sheet 3: Alternative 3' splice site (26 events)**
- **Sheet 4: Alternative 5' splice site (20 events)**
- **Sheet 5: Mutually exclusive exons (8 events)**

Dataset S4: RNAseq data of *Chd7*-null granule neuron progenitors analyzed with rMATS (253 events; inclusion level ≥ 0.1; $P < 0.05$) .

- **Sheet 1: Skipped exons (147 events)**
- **Sheet 2: Retained introns (52 events)**
- **Sheet 3: Alternative 3' splice site (26 events)**
- **Sheet 4: Alternative 5' splice site (17 events)**
- **Sheet 5: Mutually exclusive exons (11 events)**